Acta Cryst E CRYSTALLOGRAPHIC COMMUNICATIONS

ISSN 2056-9890

Crystal structure and Hirshfeld surface analysis of 4-(2-chloroethyl)-5-methyl-1,2-dihydropyrazol-3-one

Farid N. Naghiyev,[a] Victor N. Khrustalev,[b,c] Mehmet Akkurt,[d] Evgeny A. Dukhnovsky,[b] Ajaya Bhattarai,[e]* Ali N. Khalilov[f,a] and Ibrahim G. Mamedov[a]

[a]Department of Chemistry, Baku State University, Z. Khalilov str. 23, Az, 1148, Baku, Azerbaijan, [b]Peoples' Friendship University of Russia (RUDN University), Miklukho-Maklay St. 6, Moscow 117198, Russian Federation, [c]N. D. Zelinsky Institute of Organic Chemistry RAS, Leninsky Prosp. 47, Moscow, 119991, Russian Federation, [d]Department of Physics, Faculty of Sciences, Erciyes University, 38039 Kayseri, Türkiye, [e]Department of Chemistry, M.M.A.M.C (Tribhuvan University) Biratnagar, Nepal, and [f]"Composite Materials" Scientific Research Center, Azerbaijan State Economic University (UNEC), H. Aliyev str. 135, Az 1063, Baku, Azerbaijan. *Correspondence e-mail: ajaya.bhattarai@mmamc.tu.edu.np

Received 15 January 2024
Accepted 23 January 2024

Edited by X. Hao, Institute of Chemistry, Chinese Academy of Sciences

Keywords: crystal structure; hydrogen bonds; dimers; pyrazole ring; Hirshfeld surface analysis.

CCDC reference: 2327646

Supporting information: this article has supporting information at journals.iucr.org/e

In the crystal of the title compound, $C_6H_9ClN_2O$, molecular pairs form dimers with an $R_2^2(8)$ motif through N—H···O hydrogen bonds. These dimers are connect into ribbons parallel to the (100) plane with $R_4^4(10)$ motifs by N—H···O hydrogen bonds along the *c*-axis direction. In addition, π–π [centroid-to-centroid distance = 3.4635 (9) Å] and C—Cl···π interactions between the ribbons form layers parallel to the (100) plane. The three-dimensional consolidation of the crystal structure is also ensured by Cl···H and Cl···Cl interactions between these layers. According to a Hirshfeld surface study, H···H (43.3%), Cl···H/H···Cl (22.1%) and O···H/H···O (18.7%) interactions are the most significant contributors to the crystal packing.

1. Chemical context

Nitrogen-based heterocyclic compounds are an important branch of organic chemistry. These systems have received increasing attention over the past two decades. Synthetic chemistry is growing extensively with recently developed heterocyclic systems for various research and commercial purposes (Maharramov *et al.*, 2021, 2022; Erenler *et al.*, 2022; Akkurt *et al.*, 2023). These systems have found wide applications in diverse branches of chemistry, including the chemistry of coordination compounds (Gurbanov *et al.*, 2021; Mahmoudi *et al.*, 2021), drug development (Donmez & Turkyılmaz, 2022;

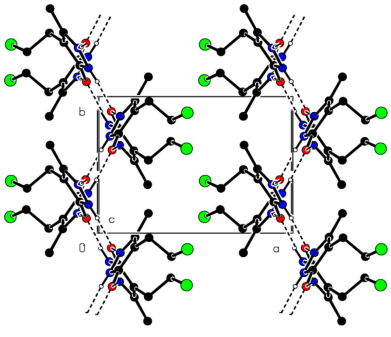

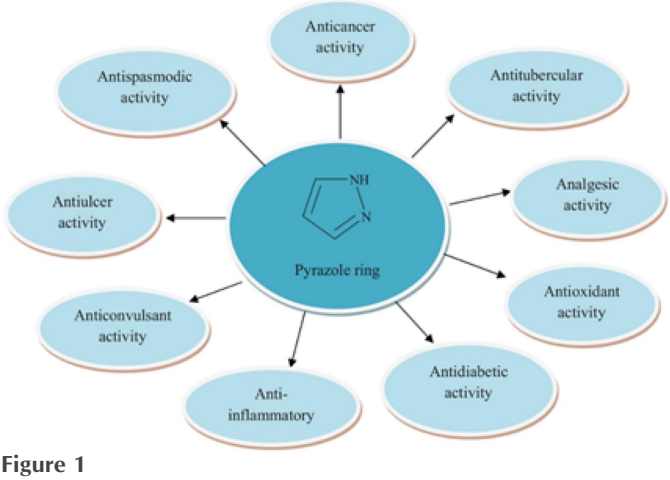

Figure 1
The biological activities of compounds incorporating the pyrazole motif.

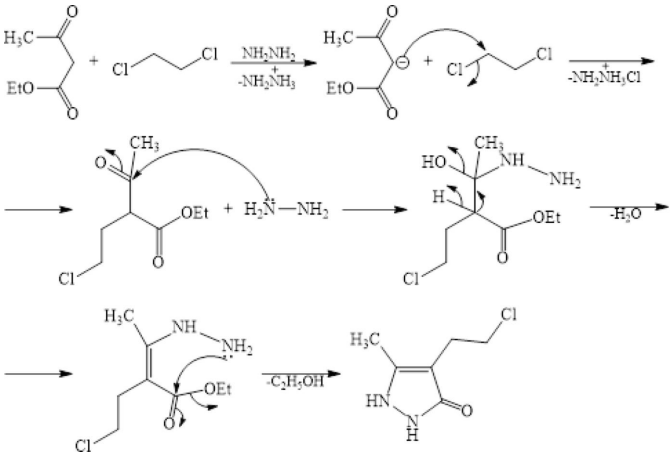

Figure 2
The proposed reaction mechanism for the formation of the title compound.

Askerova, 2022) and material science (Velásquez *et al.*, 2019; Afkhami *et al.*, 2019). The pyrazole motif is the most widespread five-membered heteroaromatic ring system in nitrogen heterocycles. It is an essential structural motif present in many natural bioactive molecules such as L-α-amino-β-(pyrazolyl-*N*)-propanoic acid, withasomnine, pyrazofurin, pyrazofurin B, formycin, formycin B, oxoformycin B, nostocine A, fluviols (A, B, C, D and E), pyrazole-3(5)-carboxylic acid, 4-*M*ethyl pyrazole-3(5)-carboxylic acid, 3-*n*-nonylpyrazole (Khalilov *et al.*, 2022; Kumar *et al.*, 2013; Sobhi & Faisal, 2023). The pyrazole ring incorporating derivatives with various biological activities (Singh *et al.*, 2023), such as anticonvulsant, antidiabetic, anti-inflammatory, antioxidant, anticancer, antitubercular, antiulcer activities and other properties has been reviewed recently (Fig. 1).

On the other hand, the incorporation of various pharmacophore groups in a pyrazole scaffold has led to the development of best-selling drugs such as ibrutinib, ruxolitinib, axitinib, niraparib and baricitinib (Atalay *et al.*, 2022; Alam, 2023). Thus, in the framework of our studies in heterocyclic chemistry (Naghiyev *et al.*, 2020, 2021, 2022), we herein report the crystal structure and Hirshfeld surface analysis of the title compound, 4-(2-chloroethyl)-5-methyl-1,2-dihydropyrazol-3-one, for which the proposed reaction mechanism is shown in Fig. 2.

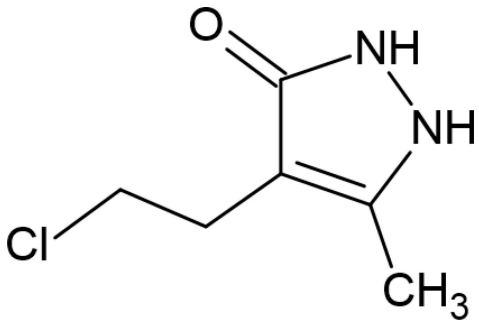

Table 1
Hydrogen-bond geometry (Å, °).

D—H···A	D—H	H···A	D···A	D—H···A
N1—H1···O1^{i}	0.88 (3)	1.81 (3)	2.6861 (18)	174 (2)
N2—H2···O1^{ii}	0.92 (3)	1.75 (3)	2.6772 (17)	177 (2)

Symmetry codes: (i) $-x, -y+2, -z+1$; (ii) $x, -y+\frac{3}{2}, z-\frac{1}{2}$.

2. Structural commentary

In the title compound (Fig. 3), the pyrazoline ring (N1/N2/C3–C5) has an essentially planar conformation [maximum deviation = 0.006 (1) Å for N1]. The C3—C4—C7—C8 and C4—C7—C8—Cl1 torsion angles are 105.67 (19) and 172.38 (11)°, respectively. The geometric parameters of the title compound are normal and comparable to those of related compounds given in the *Database survey* section.

3. Supramolecular features and Hirshfeld surface analysis

In the crystal, molecular pairs form dimers with an $R_2^2(8)$ motif (Bernstein *et al.*, 1995) through N—H···O hydrogen bonds (Table 1 and Fig. 4). These dimers are also connected into ribbons parallel to the (100) plane by forming N—H···O hydrogen bonds with $R_4^4(10)$ motifs along the *c*-axis direction (Figs. 5 and 6). In addition, π–π [$Cg1\cdots Cg1^{i}$ = 3.4635 (9) Å, slippage = 0.511 Å; symmetry code: (i) $-x, 1-y, 1-z$; $Cg1$ is a centroid of the pyrazole ring (N1/N2/C3–C5)] and C—Cl···π [C8—Cl1···$Cg1^{ii}$: C8—Cl1 = 1.8040 (18) Å, Cl1···$Cg1^{ii}$ = 3.8386 (8) Å, C8—Cl1···$Cg1^{ii}$ = 84.57 (6)°; symmetry code: (ii) $x, \frac{3}{2}-y, \frac{1}{2}+z$] interactions between the ribbons form layers parallel to the (100) plane. The three-dimensional consolidation of the crystal structure is also ensured by the Cl···H and Cl···Cl interactions [(C8)Cl1···H6B^{iii} = 3.12 (3) Å, C8—Cl1···H6B^{iii} = 135.3 (6)° and (C8)Cl1···Cl1^{iv} = 3.5071 (7) Å, C8—Cl1···Cl1^{iv} = 161.79 (7)°; symmetry codes: (iii) $1-x, \frac{1}{2}+y, \frac{3}{2}-z$; (iv) $1-x, 1-y, 2-z$] between these layers (Table 2; Fig. 7).

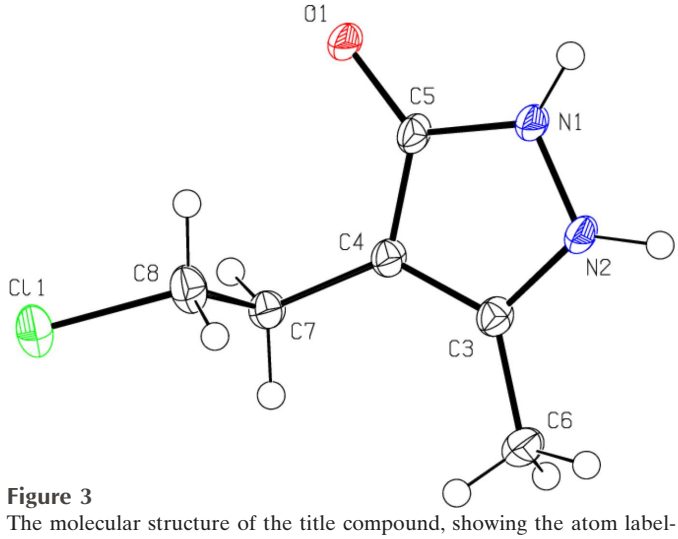

Figure 3
The molecular structure of the title compound, showing the atom labelling and displacement ellipsoids drawn at the 50% probability level.

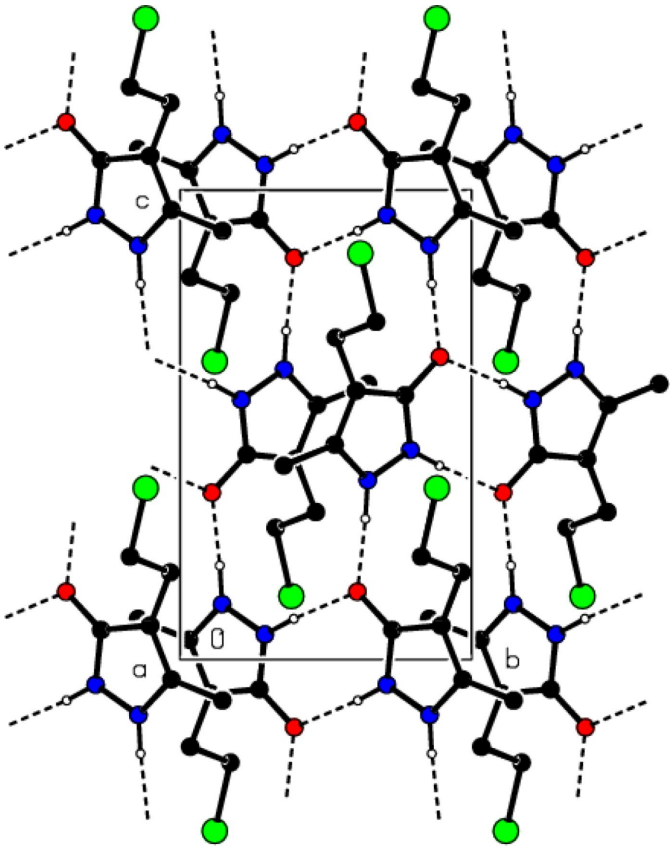

Figure 4
View of the N—H···O hydrogen bonds of the title compound down the *a*-axis.

To quantify the intermolecular interactions in the crystal, two-dimensional fingerprint plots and Hirshfeld surfaces were produced using *Crystal Explorer 17.5* (Spackman *et al.*, 2021). Fig. 8 shows the mapping of the Hirshfeld surfaces over d_{norm} in the range −0.7296 (red) to +1.3271 (blue) a.u. The interactions given in Tables 1 and 2 play a key role in the molecular packing of the title compound. H···H is the most significant interatomic contact because it contributes the most to the crystal packing (43.3%, Fig. 9*b*). Other significant contributions are made by Cl···H/H···Cl (22.1%, Fig. 9*c*) and O···H/H···O (18.7%, Fig. 9*d*) interactions. The following inter-

Table 2
Summary of short interatomic contacts (Å) in the title compound.

Cl1···H6*B*	3.12	$1-x, \frac{1}{2}+y, \frac{3}{2}-z$
Cl1···Cl1	3.51	$1-x, 1-y, 2-z$
H1···O1	1.80	$-x, 2-y, 1-z$
H6*C*···O1	2.89	$-x, 1-y, 1-z$
O1···H2	1.76	$x, \frac{3}{2}-y, \frac{1}{2}+z$
H6*A*···H7*B*	2.60	$x, \frac{1}{2}-y, -\frac{1}{2}+z$

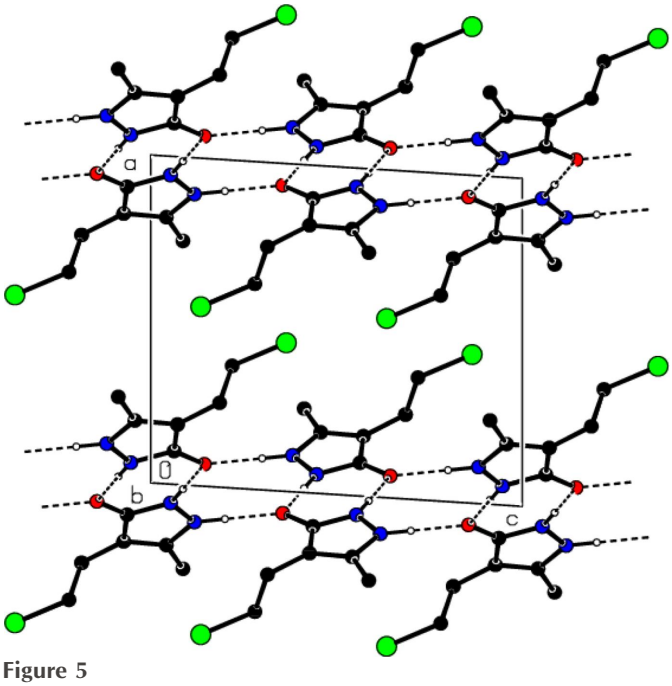

Figure 5
View of the N—H···O hydrogen bonds of the title compound down the *b*-axis.

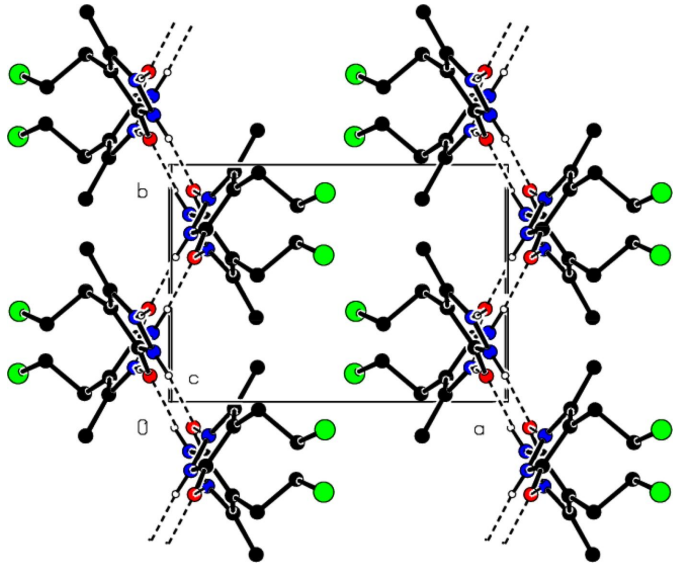

Figure 6
View of the N—H···O hydrogen bonds of the title compound down the *c*-axis.

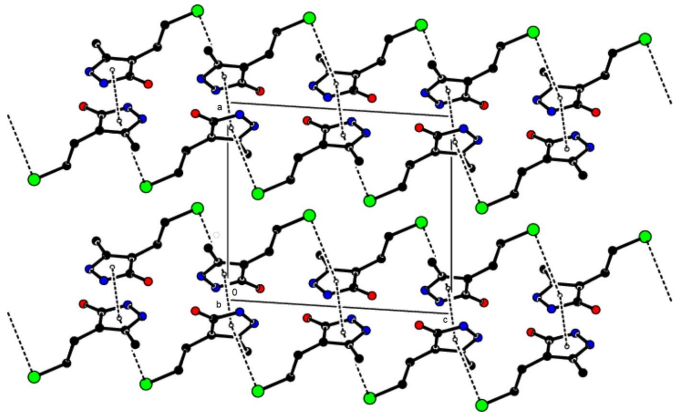

Figure 7
View of the π-π- and C—Cl···π interactions of the title compound down the *b*-axis.

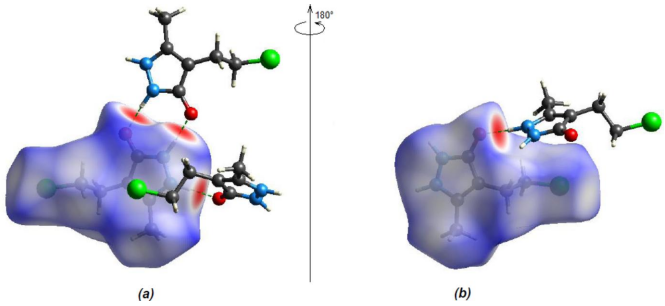

Figure 8
(*a*) Front and (*b*) back sides of the three-dimensional Hirshfeld surface of the title compound mapped over d_{norm}, with a fixed colour scale of −0.7296 to +1.3271 a.u.

actions make minor contributions: Cl···C/C···Cl (2.4%), C···H/H···C (2.6%), N···H/H···N (4.3%), N···C/C···N (3.4%), Cl···N/N···Cl (0.7%), and C···C (0.7%).

4. Database survey

A search of the Cambridge Structural Database (CSD, Version 5.43, last update November 2022; Groom *et al.*, 2016) for the central five-membered ring *2,3-dihydro-1H-pyrazole* yielded six compounds related to the title compound, *viz.* 3-methyl-5-(3-methylphenoxy)-1-phenyl-1*H*-pyrazole-4-carbaldehyde (CSD refcode TERZAV; Archana, *et al.*, 2022), *N*-{3-cyano-1-[2,6-dichloro-4-(trifluoromethyl)phenyl]-4-(ethylsulfanyl)-1*H*-pyrazol-5-yl}-2,2,2-trifluoroacetamide (FERPOL; Priyanka *et al.*, 2022), 4-[3-(4-hydroxyphenyl)-4,5-dihydro-1*H*-pyrazol-5-yl]-2-methoxyphenol monohydrate (KOXGAI; Duong Khanh *et al.*, 2019), 5-chloro-N^1-(5-phenyl-1*H*-pyrazol-3-yl)benzene-1,2-diamine (CAXZUZ; Yartsev *et al.*, 2017), 5-(butylamino)-3-methyl-1-(pyridin-2-yl)-1*H*-pyrazole-4-carbaldehyde (EYEHEX; Macías *et al.*, 2016) and 5-amino-1-(2-chlorophenyl)-1*H*-pyrazole-4-carbonitrile (AFIJOP; Lin *et al.*, 2007).

The molecular packing of TERZAV features aromatic *π*–*π* stacking and weak C—H···*π* interactions. In the crystal of FERPOL, strong N—H···O hydrogen bonds link the molecules into chains that extend parallel to the *a*-axis. In the crystal of KOXGAI, the molecules are connected into chains running in the *b*-axis direction by O—H···N hydrogen bonding. Parallel chains interact through N—H···O hydrogen bonds and *π*–*π* stacking of the trisubstituted phenyl rings. In the crystal of CAXZUZ, the *A* and *B* molecules are linked by two pairs of N—H···N hydrogen bonds, forming *A*–*B* dimers. These are further linked by a fifth N—H···N hydrogen bond, forming tetramer-like units that stack along the *a*-axis direction, forming columns, which are in turn linked by C—H···*π* interactions, forming layers parallel to the *ac* plane. The supramolecular structure of EYEHEX assembly has a three-dimensional arrangement controlled mainly by weak C—H···O and C—H···*π* interactions. The crystal structure of AFIJOP is consolidated by two N—H···N hydrogen bonds.

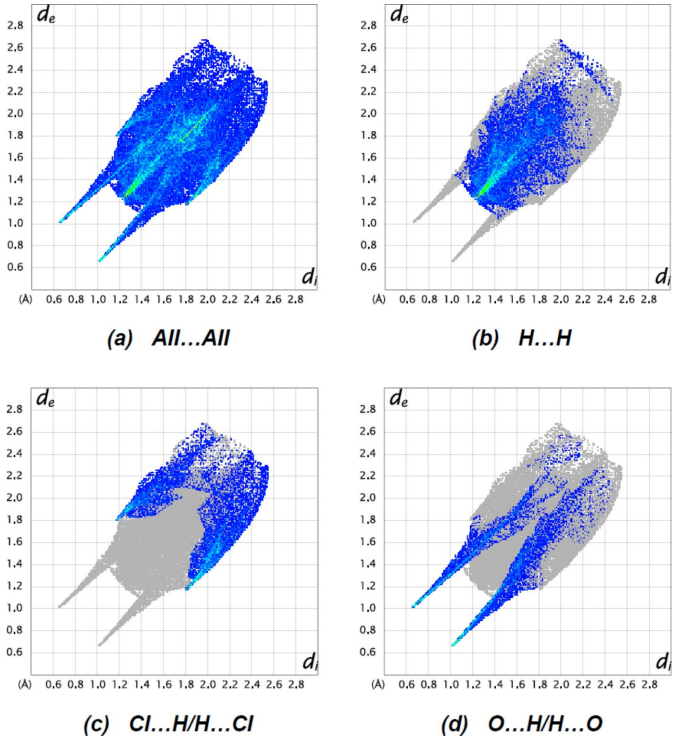

Figure 9
The two-dimensional fingerprint plots of the title compound, showing (*a*) all interactions, and delineated into (*b*) H···H, (*c*) Cl···H/H···Cl and (*d*) O···H/H···O interactions. [d_e and d_i represent the distances from a point on the Hirshfeld surface to the nearest atoms outside (external) and inside (internal) the surface, respectively].

5. Synthesis and crystallization

Acetoacetic ether (7.7 mmol), dichloroethane (7.7 mmol) and hydrazine hydrate (15.4 mmol) were dissolved in 40 ml of ethanol and the reaction mixture was refluxed for 4 h. Then the reaction mixture was cooled to room temperature with the formation of white crystals. The crystals were separated by filtration and recrystallized from an ethanol–water mixture (m.p. 499–500 K, yield 78%).

^{1}H NMR (300 MHz, DMSO-d_6, ppm.): 2.06 (*s*, 3H, CH_3); 2.64 (*t*, 2H, CH_2, $^{H\text{-}H}J_2$ = 7.2); 3.49 (*s*, 2H, 2NH); 3.58 (*t*, 2H, $ClCH_2$, $^{H\text{-}H}J_2$ = 7.2). ^{13}C NMR (75 MHz, DMSO-d_6, ppm.): 10.28 (CH_3), 26.02 (CH_2), 44.91 (CH_2Cl), 97.63 ($C_{tert.}$═), 160.12 (HN—$C_{tert.}$═), 162.34 (N—C═O).

6. Refinement

Crystal data, data collection and structure refinement details are summarized in Table 3. The C-bound H atoms were placed in calculated positions (0.95–0.99 Å) and refined as riding with U_{iso}(H) = 1.2 or 1.5U_{eq}(C). The N-bound H atoms were located in a difference map and freely refined.

Acknowledgements

Authors contributions are as follows. Conceptualization, IGM, ANK and EAD; methodology, AB and MA; investigation, VNK and FNN; writing (original draft), MA, AB and ANK;

Table 3
Experimental details.

Crystal data	
Chemical formula	$C_6H_9ClN_2O$
M_r	160.60
Crystal system, space group	Monoclinic, $P2_1/c$
Temperature (K)	100
a, b, c (Å)	9.8420 (2), 6.9145 (2), 11.1807 (2)
β (°)	93.618 (2)
V (Å^3)	759.36 (3)
Z	4
Radiation type	Cu $K\alpha$
μ (mm^{-1})	3.92
Crystal size (mm)	0.20 × 0.12 × 0.06
Data collection	
Diffractometer	XtaLAB Synergy, Dualflex, HyPix
Absorption correction	Multi-scan (*CrysAlis PRO*; Rigaku OD, 2022)
T_{min}, T_{max}	0.513, 0.750
No. of measured, independent and observed [$I > 2\sigma(I)$] reflections	6642, 1532, 1467
R_{int}	0.027
(sin $\theta/\lambda)_{max}$ (Å^{-1})	0.633
Refinement	
$R[F^2 > 2\sigma(F^2)]$, $wR(F^2)$, S	0.036, 0.097, 1.05
No. of reflections	1532
No. of parameters	127
H-atom treatment	All H-atom parameters refined
$\Delta\rho_{max}$, $\Delta\rho_{min}$ (e Å^{-3})	0.28, −0.41

Computer programs: *CrysAlis PRO* (Rigaku OD, 2022), *SHELXT* (Sheldrick, 2015*a*), *SHELXL* (Sheldrick, 2015*b*), *ORTEP-3 for Windows* (Farrugia, 2012) and *PLATON* (Spek, 2020).

writing (review and editing of the manuscript), MA and ANK; visualization, MA, IGM and FNN; funding acquisition, VNK, AB and FNN; resources, AB, VNK and MA; supervision, MA and ANK.

Funding information

This paper was supported by Baku State University and the RUDN University Strategic Academic Leadership Program.

References

Afkhami, F. A., Mahmoudi, G., Khandar, A. A., Franconetti, A., Zangrando, E., Qureshi, N., Lipkowski, J., Gurbanov, A. V. & Frontera, A. (2019). *Eur. J. Inorg. Chem.* pp. 262–270.
Akkurt, M., Maharramov, A. M., Shikhaliyev, N. G., Qajar, A. M., Atakishiyeva, G., Shikhaliyeva, I. M., Niyazova, A. A. & Bhattarai, A. (2023). *UNEC J. Eng. Appl. Sci.* **3**, 33–39.
Alam, M. A. (2023). *Future Med. Chem.* **15**, 2011–2023.
Archana, S. D., Nagma Banu, H. A., Kalluraya, B., Yathirajan, H. S., Balerao, R. & Butcher, R. J. (2022). *IUCrData*, **7**, x220924.
Askerova, U. F. (2022). *UNEC J. Eng. Appl. Sci*, **2**, 58–64.
Atalay, V. E., Atish, I. S., Shahin, K. F., Kashikchi, E. S. & Karahan, M. (2022). *UNEC J. Eng. Appl. Sci.* **2**, 33–40.
Bernstein, J., Davis, R. E., Shimoni, L. & Chang, N.-L. (1995). *Angew. Chem. Int. Ed. Engl.* **34**, 1555–1573.
Donmez, M. & Turkyılmaz, M. (2022). *UNEC J. Eng. Appl. Sci*, **2**, 43–48.
Duong Khanh, L., Hanh Trinh Thi, M., Quynh Bui Thi, T., Vu Quoc, T., Nguyen Thien, V. & Van Meervelt, L. (2019). *Acta Cryst.* E**75**, 1590–1594.
Erenler, R., Dag, B. & Ozbek, B. B. (2022). *UNEC J. Eng. Appl. Sci.* **2**, 26–32.
Farrugia, L. J. (2012). *J. Appl. Cryst.* **45**, 849–854.
Groom, C. R., Bruno, I. J., Lightfoot, M. P. & Ward, S. C. (2016). *Acta Cryst.* B**72**, 171–179.
Gurbanov, A. V., Mertsalov, D. F., Zubkov, F. I., Nadirova, M. A., Nikitina, E. V., Truong, H. H., Grigoriev, M. S., Zaytsev, V. P., Mahmudov, K. T. & Pombeiro, A. J. L. (2021). *Crystals*, **11**, 112.
Khalilov, A. N., Khrustalev, V. N., Tereshina, T. A., Akkurt, M., Rzayev, R. M., Akobirshoeva, A. A. & Mamedov, İ. G. (2022). *Acta Cryst.* E**78**, 525–529.
Kumar, V., Kaur, K., Gupta, G. K. & Sharma, A. K. (2013). *Eur. J. Med. Chem.* **69**, 735–753.
Lin, Q.-L., Zhong, P. & Hu, M.-L. (2007). *Acta Cryst.* E**63**, o3813.
Macías, M. A., Orrego-Hernández, J. & Portilla, J. (2016). *Acta Cryst.* E**72**, 1672–1674.
Maharramov, A. M., Shikhaliyev, N. G., Zeynalli, N. R., Niyazova, A. A., Garazade, Kh. A. & Shikhaliyeva, I. M. (2021). *UNEC J. Eng. Appl. Sci.* **1**, 5–11.
Maharramov, A. M., Suleymanova, G. T., Qajar, A. M., Niyazova, A. A., Ahmadova, N. E., Shikhaliyeva, I. M., Garazade, Kh. A., Nenajdenko, V. G. & Shikaliyev, N. G. (2022). *UNEC J. Eng. Appl. Sci.* **2**, 64–73.
Mahmoudi, G., Zangrando, E., Miroslaw, B., Gurbanov, A. V., Babashkina, M. G., Frontera, A. & Safin, D. A. (2021). *Inorg. Chim. Acta*, **519**, 120279.
Naghiyev, F. N., Akkurt, M., Askerov, R. K., Mamedov, I. G., Rzayev, R. M., Chyrka, T. & Maharramov, A. M. (2020). *Acta Cryst.* E**76**, 720–723.
Naghiyev, F. N., Khrustalev, V. N., Novikov, A. P., Akkurt, M., Rzayev, R. M., Akobirshoeva, A. A. & Mamedov, I. G. (2022). *Acta Cryst.* E**78**, 554–558.
Naghiyev, F. N., Tereshina, T. A., Khrustalev, V. N., Akkurt, M., Rzayev, R. M., Akobirshoeva, A. A. & Mamedov, İ. G. (2021). *Acta Cryst.* E**77**, 516–521.
Priyanka, P., Jayanna, B. K., Sunil Kumar, Y. C., Shreenivas, M. T., Srinivasa, G. R., Divakara, T. R., Yathirajan, H. S. & Parkin, S. (2022). *Acta Cryst.* E**78**, 1084–1088.
Rigaku OD (2022). *CrysAlis PRO*. Rigaku Oxford Diffraction, Yarnton, England.
Sheldrick, G. M. (2015*a*). *Acta Cryst.* A**71**, 3–8.
Sheldrick, G. M. (2015*b*). *Acta Cryst.* C**71**, 3–8.
Singh, S., Tehlan, S. & Kumar Verma, P. (2023). *Mini Rev. Med. Chem.* **23**, 2142–2165.
Sobhi, R. M. & Faisal, R. M. (2023). *UNEC J. Eng. Appl. Sci.* **3**, 21–32.
Spackman, P. R., Turner, M. J., McKinnon, J. J., Wolff, S. K., Grimwood, D. J., Jayatilaka, D. & Spackman, M. A. (2021). *J. Appl. Cryst.* **54**, 1006–1011.
Spek, A. L. (2020). *Acta Cryst.* E**76**, 1–11.
Velásquez, J. D., Mahmoudi, G., Zangrando, E., Gurbanov, A. V., Zubkov, F. I., Zorlu, Y., Masoudiasl, A. & Echeverría, J. (2019). *CrystEngComm*, **21**, 6018–6025.
Yartsev, Y., Palchikov, V., Gaponov, A. & Shishkina, S. (2017). *Acta Cryst.* E**73**, 876–879.

supporting information

Acta Cryst. (2024). E**80**, 223-227 [https://doi.org/10.1107/S2056989024000835]

Crystal structure and Hirshfeld surface analysis of 4-(2-chloroethyl)-5-methyl-1,2-dihydropyrazol-3-one

Farid N. Naghiyev, Victor N. Khrustalev, Mehmet Akkurt, Evgeny A. Dukhnovsky, Ajaya Bhattarai, Ali N. Khalilov and İbrahim G. Mamedov

Computing details

4-(2-Chloroethyl)-5-methyl-1,2-dihydropyrazol-3-one

Crystal data

$C_6H_9ClN_2O$
M_r = 160.60
Monoclinic, $P2_1/c$
a = 9.8420 (2) Å
b = 6.9145 (2) Å
c = 11.1807 (2) Å
β = 93.618 (2)°
V = 759.36 (3) Å^3
Z = 4
$F(000)$ = 336
D_x = 1.405 Mg m^{-3}
Cu $K\alpha$ radiation, λ = 1.54184 Å
Cell parameters from 4592 reflections
θ = 4.5–77.6°
μ = 3.92 mm^{-1}
T = 100 K
Prism, colourless
0.20 × 0.12 × 0.06 mm

Data collection

XtaLAB Synergy, Dualflex, HyPix diffractometer
Radiation source: micro-focus sealed X-ray tube
ω scans
Absorption correction: multi-scan (CrysAlisPro; Rigaku OD, 2022)
T_{min} = 0.513, T_{max} = 0.750
6642 measured reflections
1532 independent reflections
1467 reflections with $I > 2\sigma(I)$
R_{int} = 0.027
θ_{max} = 77.5°, θ_{min} = 4.5°
h = −12→12
k = −8→7
l = −14→8

Refinement

Refinement on F^2
Least-squares matrix: full
$R[F^2 > 2\sigma(F^2)]$ = 0.036
$wR(F^2)$ = 0.097
S = 1.05
1532 reflections
127 parameters
0 restraints
Primary atom site location: difference Fourier map
Secondary atom site location: difference Fourier map
Hydrogen site location: difference Fourier map
All H-atom parameters refined
$w = 1/[\sigma^2(F_o^2) + (0.0501P)^2 + 0.606P]$ where $P = (F_o^2 + 2F_c^2)/3$
$(\Delta/\sigma)_{max}$ = 0.001
$\Delta\rho_{max}$ = 0.28 e Å^{-3}
$\Delta\rho_{min}$ = −0.41 e Å^{-3}

Special details

Geometry. All esds (except the esd in the dihedral angle between two l.s. planes) are estimated using the full covariance matrix. The cell esds are taken into account individually in the estimation of esds in distances, angles and torsion angles; correlations between esds in cell parameters are only used when they are defined by crystal symmetry. An approximate (isotropic) treatment of cell esds is used for estimating esds involving l.s. planes.

Fractional atomic coordinates and isotropic or equivalent isotropic displacement parameters (Å²)

	x	*y*	*z*	U_{iso}*/U_{eq}
Cl1	0.45324 (5)	0.61848 (7)	0.86496 (4)	0.03447 (18)
O1	0.06705 (13)	0.89161 (17)	0.64445 (10)	0.0231 (3)
N1	0.05777 (14)	0.7905 (2)	0.44644 (12)	0.0197 (3)
H1	0.013 (3)	0.890 (4)	0.413 (2)	0.040 (7)*
N2	0.11129 (14)	0.6437 (2)	0.38217 (12)	0.0195 (3)
H2	0.096 (2)	0.636 (3)	0.300 (2)	0.038 (6)*
C3	0.18687 (16)	0.5302 (2)	0.45765 (14)	0.0189 (3)
C4	0.18362 (16)	0.6035 (2)	0.57245 (14)	0.0181 (3)
C5	0.10154 (16)	0.7717 (2)	0.56311 (13)	0.0188 (3)
C6	0.2560 (2)	0.3553 (3)	0.41307 (16)	0.0254 (4)
H6A	0.282 (3)	0.372 (4)	0.331 (3)	0.058 (8)*
H6B	0.338 (3)	0.328 (5)	0.458 (3)	0.065 (9)*
H6C	0.205 (3)	0.250 (5)	0.414 (3)	0.066 (9)*
C7	0.25721 (17)	0.5342 (2)	0.68559 (14)	0.0205 (3)
H7A	0.194 (2)	0.527 (3)	0.7508 (18)	0.021 (5)*
H7B	0.295 (2)	0.406 (3)	0.676 (2)	0.029 (5)*
C8	0.37260 (18)	0.6724 (3)	0.71941 (16)	0.0254 (4)
H8A	0.340 (2)	0.807 (4)	0.724 (2)	0.031 (6)*
H8B	0.443 (2)	0.665 (4)	0.664 (2)	0.037 (6)*

Atomic displacement parameters (Å²)

	U^{11}	U^{22}	U^{33}	U^{12}	U^{13}	U^{23}
Cl1	0.0401 (3)	0.0366 (3)	0.0249 (3)	0.00431 (18)	−0.01242 (19)	−0.00157 (17)
O1	0.0374 (7)	0.0209 (6)	0.0110 (5)	0.0082 (5)	0.0007 (5)	−0.0010 (4)
N1	0.0297 (7)	0.0180 (7)	0.0114 (6)	0.0045 (5)	0.0008 (5)	−0.0006 (5)
N2	0.0278 (7)	0.0194 (7)	0.0115 (7)	0.0026 (5)	0.0013 (5)	−0.0028 (5)
C3	0.0237 (7)	0.0179 (7)	0.0153 (7)	−0.0011 (6)	0.0027 (6)	0.0008 (6)
C4	0.0238 (7)	0.0177 (7)	0.0128 (7)	0.0008 (6)	0.0024 (6)	0.0017 (6)
C5	0.0273 (8)	0.0183 (7)	0.0110 (7)	−0.0002 (6)	0.0023 (6)	0.0003 (6)
C6	0.0333 (9)	0.0233 (8)	0.0198 (9)	0.0057 (7)	0.0033 (7)	−0.0036 (7)
C7	0.0280 (8)	0.0192 (8)	0.0144 (8)	0.0036 (6)	0.0015 (6)	0.0016 (6)
C8	0.0264 (8)	0.0315 (9)	0.0180 (8)	0.0006 (7)	−0.0019 (6)	0.0029 (7)

Geometric parameters (Å, º)

Cl1—C8	1.8040 (18)	C4—C7	1.496 (2)
O1—C5	1.2920 (19)	C6—H6A	0.97 (3)
N1—C5	1.354 (2)	C6—H6B	0.95 (3)

N1—N2	1.3685 (19)	C6—H6C	0.88 (3)
N1—H1	0.88 (3)	C7—C8	1.514 (2)
N2—C3	1.342 (2)	C7—H7A	0.99 (2)
N2—H2	0.92 (3)	C7—H7B	0.97 (2)
C3—C4	1.382 (2)	C8—H8A	0.99 (2)
C3—C6	1.489 (2)	C8—H8B	0.95 (2)
C4—C5	1.416 (2)		

C5—N1—N2	108.95 (13)	H6A—C6—H6B	105 (2)
C5—N1—H1	126.8 (17)	C3—C6—H6C	113 (2)
N2—N1—H1	123.6 (17)	H6A—C6—H6C	107 (3)
C3—N2—N1	108.66 (13)	H6B—C6—H6C	107 (3)
C3—N2—H2	129.9 (15)	C4—C7—C8	108.91 (14)
N1—N2—H2	121.4 (15)	C4—C7—H7A	110.2 (12)
N2—C3—C4	108.96 (14)	C8—C7—H7A	110.3 (12)
N2—C3—C6	120.74 (15)	C4—C7—H7B	111.5 (13)
C4—C3—C6	130.29 (15)	C8—C7—H7B	108.6 (13)
C3—C4—C5	106.22 (14)	H7A—C7—H7B	107.3 (18)
C3—C4—C7	128.97 (15)	C7—C8—Cl1	112.04 (12)
C5—C4—C7	124.69 (14)	C7—C8—H8A	111.5 (13)
O1—C5—N1	122.31 (15)	Cl1—C8—H8A	105.7 (13)
O1—C5—C4	130.49 (14)	C7—C8—H8B	111.5 (15)
N1—C5—C4	107.19 (13)	Cl1—C8—H8B	106.1 (15)
C3—C6—H6A	111.6 (17)	H8A—C8—H8B	109.7 (19)
C3—C6—H6B	111.9 (19)		

C5—N1—N2—C3	0.98 (18)	N2—N1—C5—C4	−1.24 (18)
N1—N2—C3—C4	−0.30 (18)	C3—C4—C5—O1	179.99 (17)
N1—N2—C3—C6	178.79 (15)	C7—C4—C5—O1	−3.7 (3)
N2—C3—C4—C5	−0.45 (18)	C3—C4—C5—N1	1.04 (18)
C6—C3—C4—C5	−179.43 (17)	C7—C4—C5—N1	177.36 (15)
N2—C3—C4—C7	−176.56 (16)	C3—C4—C7—C8	105.67 (19)
C6—C3—C4—C7	4.5 (3)	C5—C4—C7—C8	−69.8 (2)
N2—N1—C5—O1	179.70 (15)	C4—C7—C8—Cl1	172.38 (11)

Hydrogen-bond geometry (Å, º)

D—H···*A*	*D*—H	H···*A*	*D*···*A*	*D*—H···*A*
N1—H1···O1^{i}	0.88 (3)	1.81 (3)	2.6861 (18)	174 (2)
N2—H2···O1^{ii}	0.92 (3)	1.75 (3)	2.6772 (17)	177 (2)

Symmetry codes: (i) −*x*, −*y*+2, −*z*+1; (ii) *x*, −*y*+3/2, *z*−1/2.